Journal of Ethnopharmacology 153 (2014) 604–614

Contents lists available at ScienceDirect

Journal of Ethnopharmacology

journal homepage: www.elsevier.com/locate/jep

Research Paper

Immunopotentiation of *Pleurotus eryngii* (DC. ex Fr.) Quel

Alfred Mugambi Mariga [a,b], Fei Pei [a], Wen-jian Yang [c], Li-yan Zhao [a], Ya-ni Shao [a], Dorothy Kemuma Mugambi [d], Qiu-hui Hu [a,*]

[a] College of Food Science and Technology, Nanjing Agricultural University, No. 1 Weigang Road, Nanjing 210095, PR China
[b] Department of Dairy and Food Science and Technology, Egerton University, Egerton 536, Kenya
[c] College of Food Science and Engineering, Nanjing University of Finance and Economics, No. 3 Wenyuan Road, Nanjing 210046, PR China
[d] College of Resources and Environmental Sciences, Nanjing Agricultural University, No. 1 Weigang Road, Nanjing 210095, PR China

ARTICLE INFO

Article history:
Received 8 November 2013
Received in revised form
19 January 2014
Accepted 1 March 2014
Available online 18 March 2014

Keywords:
Extraction
Cytotoxicity
Immumodulation
Pleurotus eryngii (DC. ex Fr.) Quel powder

ABSTRACT

Ethnopharmacological relevance: *Pleurotus eryngii* (DC. ex Fr.) Quel has been collected from the wild, cultivated and used in traditional medicines to treat various disorders and diseases since antiquity. In traditional Chinese medicine, the powdered fruiting bodies of *Pleurotus eryngii* were used for immunostimulation, skin-care, wound-healing, cancer and lumbago treatment. In the current study, we investigated the antiproliferative activity of *Pleurotus eryngii* powder on A549, BGC-823, HepG2 and HGC-27 cancer cells and its immunomodulating activity on macrophage, RAW 264.7 cells based on its active compound.

Materials and methods: A novel bioactive protein (PEP) was extracted from *Pleurotus eryngii* fruiting bodies powder and purified on DEAE-52, CM-52 and Superdex 75 column chromatographies using an ÄKTA purifier. Its cytotoxicity on A549, BGC-823, HepG2, HGC-27 and RAW 267.4 cell lines was then evaluated using MTT, alamar blue (AB), trypan blue (TB), neutral red (NR), lactate dehydrogenase (LDH), Annexin V FITC/PI and morphological change assays. Moreover, lysosomal enzyme activity, pinocytosis, nitric oxide (NO) and hydrogen peroxide (H_2O_2) production assays were used to examine immunomostimulatory activity of PEP on RAW 267.4 cells.

Results: Based on high performance gel permeation chromatography (HPGPC), Fourier transform infrared (FT-IR) and nuclear magnetic resonance (NMR) analyses, the isolated protein (PEP) had a molecular weight of 63 kDa, a secondary (α-helical) structure and was mainly composed of arginine, serine and glycine. PEP significantly ($P < 0.05$) inhibited A549, BGC-823, HepG2 and HGC-27 tumor cells proliferation dose-dependently with an IC_{50} range of 36.5 ± 0.84 to 229.0 ± 1.24 μg/ml. Contrarily, PEP stimulated the proliferation of macrophages.

Conclusion: *Pleurotus eryngii* fruiting bodies powder has a potential application as a natural antitumor agent with immunomodulatory activity, proposedly, by targeting the lysosomes of cancerous cells and stimulating macrophage-mediated immune responses.

1. Introduction

For millennia, humankind has valued mushrooms as an important edible and medical resource (Fujita et al., 2005; Synytsya et al., 2009). Currently, mushroom-derived substances with antitumor and immunomodulating properties are used as dietary supplements or drugs (Yang et al., 2013). Most of the cultivated medicinal mushrooms such as *Ganoderma lucidum*, *Lentinus edodes* (Shiitake) and *Pleurotus* species have been collected and used for centuries in Korea, China, Japan and eastern Russia for food, phytomedicine and functional food (Fujita et al., 2005; Synytsya et al., 2009; Yang et al., 2013). Mushrooms from *Pleurotus* species have been demonstrated to possess many medicinal functions including hepatoprotective and hypolipidemic (Wasser and Weis, 1999; Wasser, 2002; Chen et al., 2012), antioxidant (Synytsya et al., 2009), antitumor (Yang et al., 2013) and immunomodulating activities (Jeong et al., 2010). *Pleurotus eryngii* (DC. ex Fr.) Quel, a well-known culinary-medicinal mushroom is generally grown on a wide range of lignocellulosic materials (Liang et al., 2011). *Pleurotus eryngii* is a typical component of the Mediterranean mycoflors. It grows in close association with umbelifers and produces highly priced edible mushrooms. It was first artificially cultivated in the USA, though production is now worldwide (Wasser, 2002). *Pleurotus eryngii* has an established history of use in traditional oriental medicine, where most of its preparations are regarded as tonics, that is, they have beneficial health effects without known negative side-effects and can apparently be used moderately on

* Corresponding author. Tel.: +86 13951745468; fax: +86 25 84399086.
E-mail address: qiuhuihu@njau.edu.cn (Q.-h. Hu).

http://dx.doi.org/10.1016/j.jep.2014.03.006
0378-8741/

a regular basis without harm (Hobbs, 1995; Wasser and Weis, 1999). *Pleurotus eryngii* has been used in traditional medicine for at least 35 disorders or diseases. In china, it was referred to as "the mushroom of flower heaven" in the Sung dynasty (A.D. 420–479) and it was recommended in Chinese traditional medicine for preparing an invigorating and immune stimulating tea (immune tonic) (Hobbs, 1995; Mizuno, 1995; Chang, 1999). It was also used for treating debility and exhaustion as well as many other ailments including skin-care, wounds and for joint and muscle relaxation (Hobbs, 1995). Moreover, the powdered fruiting bodies of *Pleurotus eryngii* were used as effective cancer, lumbago, numbed limbs and tendon and blood vessel discomfort treatment (Wiel, 1987; Wasser and Weis, 1999). The medicinally beneficial effects of the *Pleurotus* species were discovered independently in different continents, hence, the awareness of their medicinal properties comes not only from Asia but from the folklore of central Europe, South America and Africa (Gunde-Cimerman, 1999; Wasser, 2002). The historical usage of this medicinal mushroom was mostly as a whole mushroom, hot water extract, concentrate, liquor or powder and it was used directly, in health tonics, tinctures, teas, soups or herbal formulae (Mizuno et al., 1995; Gunde-Cimerman, 1999; Wasser, 2002). Previous pharmacological studies have confirmed the cytotoxic activity of the extracts, concentrates, liquors, powders and purified macromolecules including protein from *Pleurotus eryngii* on various human carcinomas. Their immunostimulation ability in splenocytes and NK cells has been reported. However, the antiproliferative activity of the powder from the fruiting bodies of *Pleurotus eryngii* on A549, BGC-823, HepG2 and HGC-27 cells and its immunostimulation ability in macrophages, RAW 264.7 cells has not been reported. Thus, a dose-dependent cytotoxicity of the *Pleurotus eryngii* fruiting bodies powder (based on the active component, a protein; PEP), on A549, BGC-823, HepG2 and HGC-27 cancer cells and its immunomodulating activity on macrophage, RAW 264.7 cells have been reported in the present study.

2. Materials and methods

2.1. Plant material

Fruiting bodies of *Pleurotus eryngii* (DC. ex Fr.) Quel were purchased from a local market (Nanjing, P.R. China). The fruits were washed in water, dried at room temperature to constant weight and then ground to pass through 80 mesh screen. The powder obtained was stored at 4 °C until used.

2.2. Cell lines

The non-small cell lung cancer A549 (NSCLC), human stomach adenocarcinoma BGC-823, human liver hepatocellular carcinoma HepG2, human gastric carcinoma HGC-27 and macrophage RAW 264.7 cell lines were obtained from State Key Laboratory of Pharmaceutical Biotechnology, School of Life Sciences, Nanjing University (Nanjing, P.R. China). They were maintained in Dulbecco's Modified Eagle medium (DMEM) (Gibco, NY, USA) supplemented with 10% fetal bovine serum (FBS) and 1% Pen Strep (Gibco) at 37 °C in a humidified incubator (Thermo Scientific, Marietta, USA) with 5% carbon dioxide (CO_2).

2.3. Chemicals

Alamar blue dye was purchased from Invitrogen (NY, USA) while trypan blue (TB) dye, dimethyl sulfoxide (DMSO), Griess reagent and Superdex 75 column were purchased from Sigma-Aldrich Co. (St. Louis, MO, USA). Positive controls; paclitaxel (PTX) for A549, doxorubicin (Dox) for BGC-823 and HepG2, mitomycin C (MMC), HGC-27 and lipopolysaccharide (LPS) for RAW 264.7 cells respectively, were purchased from Kayon Biological technology Co. Ltd (Shanghai, P.R. China). Bovine serum albumin (BSA), phosphate buffered saline (PBS, pH 7.4) and 3-(4,5-dimethylthiazole-2-yl)-2,5-dimethyltetrazolium bromide (MTT) were purchased from Gibco. Preswollen diethylaminoethyl cellulose (DEAE-52) and carboxymethyl cellulose (CM-52) columns were obtained from Whatman (Kent, UK), while 0.22 and 0.45 μm filters were from Millipore Co. (Bedford, UK). All other chemicals and reagents used were of analytical grade, and were purchased from Shanghai Chemical Reagent Co. (Shanghai, P.R. China).

2.3.1. Protein extraction from Pleurotus eryngii fruiting bodies

The protein was isolated and purified according to the method described by Chang et al. (2007) with slight modification. Briefly, the powdered fruiting bodies of *Pleurotus eryngii*, approximately 150 g were homogenized in 3000 ml ice-cold 5% acetic acid and the homogenate was centrifuged (Model: TDL-5-A, Shanghai, P.R. China) at 5000 rpm for 30 min. The soluble protein in the supernatant was subsequently precipitated overnight by saturated (95%) ammonium sulfate ($(NH4)_2SO_4$) at 4 °C. Centrifugation at 5000 rpm for 35 min followed and the pellets obtained were pooled, solubilized in de-ionized water and dialyzed at 4 °C for 24 h against de-ionized water using 10 kDa molecular weight cut-off dialysis membranes. Consequently, the dialysate was lyophilized to obtain crude protein (CP) fraction. The protein concentration of the CP was ultimately determined by the Bradford (1976) method using BSA as the standard.

2.3.2. Purification

Preswollen DEAE-52 resin was pretreated and packed into a 2.6 × 30 cm (inside diameter (id) × length (l)) Bio-Rad column. The column was subsequently equilibrated with three column volumes (CV) of 10 mM tris(hydroxymethyl)-aminomethane/hydrochloric acid (Tris–HCl, pH 8.0) buffer at a flow rate of 0.8 ml/min. Five-hundred milligrams of crude protein was dissolved in 5 ml Tris–HCl buffer, applied to the column and was eluted with 200 ml of the buffer. Following the removal of the unadsorbed fraction, the column was successively eluted with a linear 0–0.5 M NaCl gradient in the starting buffer (Tris–HCl) and the column effluent was collected using a fraction collector. All fractions were monitored for the protein presence at 280 nm using a UV Bluestar A spectrophotometer (Shanghai, P.R. China). From the elution pattern, the absorption peaks were collected, pooled, dialyzed against de-ionized water and lyophilized (Labconco, Kansas, USA) before quantification of the protein content. The active fraction (DE 2) was further applied to CM-52 column and was eluted with a linear gradient of 0–0.5 M NaCl in 10 mM NH_4OAc buffer (pH 4.6) at 0.8 ml/min. The unadsorbed fraction was eluted with the buffer and was collected as fraction CM 1. Fraction CM 1 (active) was finally purified by gel filtration on a Superdex 75 column using an ÄKTA Purifier System (GE Healthcare, Sweden) in 0.2 M NH_4HCO_3 buffer (pH 8.5) at 1.0 ml/min. A single peak (SU) was obtained, which was eventually dialyzed, lyophilized, and designated as PEP. PEP was then stored at −20 °C until used.

2.3.3. Homogeneity and molecular weight determination

The homogeneity and molecular weight of PEP was determined by high-performance gel-permeation chromatography (HPGPC), which was performed on a Agilent 1200 series system (Agilent Technologies, Waldbronn, Germany) fitted with a TSKgel-G4000PW_{XL} column (7.8 × 300 mm) (TOSOH Corp., Tokyo, Japan). PEP was dissolved in de-ionized water (2 mg/ml), passed through a 0.45 μm filter, injected (20 μl) for HPGPC analysis and was eluted with acetonitrile/TFA (100% CH_3CN in 0.1% TFA, v/v) at 0.3 ml/min

at 25 °C. The molecular mass was estimated by reference to a calibration curve which was obtained from a series of standard proteins; aprotonin (6.5 kDa), glutamic dehydrogenase (36 kDa), ovalbumin (45 kDa), albumin bovine serum (66 kDa) and blue dextran (200 kDa) following the method described by Zhou et al. (2013).

2.3.4. Fourier transform infrared (FT-IR) and nuclear magnetic resonance (NMR) characterization of PEP

The purified protein was characterized using a FT-IR spectrophotometer (Nexus-870 Thermo-Nickolet, Madison, USA). Briefly, the freeze-dried protein was ground with potassium bromide (KBr) powder at a ratio of 1:50 and pressed into discs of halide salt for FT-IR spectral measurement in the frequency range of 4000–400 cm^{-1}. For ^1H NMR study, PEP (30 mg) was dissolved in D_2O (0.6 ml), centrifuged to remove undissolved particles and all spectra were recorded on a Bruker Avance III 400 NMR (Bruker Biospin, Rheinstetten, Germany). Chemical shift was expressed in ppm.

2.4. in vitro cytotoxicity evaluation

2.4.1. MTT assay

The IC_{50} of PEP and the positive controls was generated from the dose–response curves for each tumor cell line using the MTT colorimetric assay method developed by Mosmann (1983). The obtained IC_{50} values, 0, 40 (lowest) and 320 (highest) μg/ml were subsequently used throughout the study.

Cells were harvested from the maintenance cultures in their exponential growth phase and 100 μl of the cell suspension was inoculated into each well of 96-well plates (Corning Co., NY, USA) at a density of 2×10^5 cells/ml. After 24-h growth period to subconfluent state, the medium was aspirated and replaced with 100 μl of PEP (at 0–320 μg/ml and 0–160 μg/ml for tumor and RAW 264.7 cell lines respectively) and positive controls, followed by incubation at 37 °C, 5% CO_2 for additional 24 h. The supernatant was discarded and 100 μl MTT solution (5 mg/ml prepared in PBS and filtered through a 0.22 μm Millipore filter) was added. The supernatant was discarded after 2 h of incubation and 100 μl of DMSO was added to solubilize the formed formazan crystals. After shaking the plates for 10 min, the absorbance (Abs.) of each well was read at 570 nm by a uQuant ELISA analyzer (BioTek Instruments, Winooski, USA). Cell viability was expressed as a percentage of alive cells and the data was presented as mean ± standard deviation (SD) from three independent experiments ($n=6$ replicates per sample in each experiment). The cell viability was calculated as

$$\text{Viability}(\%) = (\text{Abs.experimental group}/\text{Abs.blank control group}) \times 100\% \quad (1)$$

2.4.2. Alamar blue (AB) cell viability assay

This assay was carried out according to the method described by Mukherjee et al. (2012) with slight modification. After treating the tumor cells with the predetermined IC_{50} values, 40 and 320 μg/ml of PEP (or 0–160 μg/ml PEP for macrophages), 10 μl (1/10th volume) of oxidized alamar blue (AB) dye was directly added to the cells (100 μl) in the culture medium to indicate cytosol integrity. Afterwards, the cells were incubated for 2 h and the absorbance of the reduced dye was monitored at 570 nm, using 600 nm as a reference wavelength. To calculate the cell viability after treatment, the abovementioned Eq. (1) was used.

2.4.3. Trypan blue (TB) dye exclusion assay

Plasma membrane integrity was evaluated through trypan blue dye exclusion assay according to the method described by Pareek et al. (2013) with modifications. A half ml aliquot of cell suspension (obtained from treated and non-treated cells), was mixed with 0.5 ml of 0.4% TB dye and left for 5 min at room temperature. The cells were later counted in a haemocytometer under an inverted light microscope (Nikon Eclipse TS100, Japan) and categorized as alive (transparent and clear) or dead (stained blue). The percentage of cellular integrity was then calculated for each treatment condition as;

$$\text{Viability}(\%) = (\text{Number of viable cells}/\text{Total number of cells}) \times 100\% \quad (2)$$

2.4.4. Neutral red (NR) uptake

The NR uptake assay was evaluated as described by Taner et al. (2013) with some modifications. After treatment, the medium was replaced with 0.1 ml of DMEM per well containing 1% (v/v) NR, and the plates were re-incubated for 3 h to allow the lysosomes of viable cells to take up the dye. The incorporated dye was then eluted from the cells by adding 0.1 ml elution medium (50% ethanol, 49% de-ionized water and 1% acetic acid, v- v- v) into each well followed by gentle shaking for 10 min. The absorbance was read at 540 nm and the results were expressed as a percent of the untreated cells using Eq. (1) above.

2.4.5. Determination of LDH release

Toxicity of PEP to the various cell lines was determined by the release of lactate dehydrogenase (LDH) into the culture medium as described by Biswas et al. (2013) with modifications. Approximately 2×10^5 cells/ml were plated onto each well of a 96-well plate and the plates were incubated for 24 h. Cells were then treated with PEP or control and incubated for 24 h. Following exposure to PEP, the culture medium was aspirated and centrifuged at 3000 rpm for 5 min to obtain a cell free supernatant. The supernatant (20 μl) from each sample was pipetted in triplicate into the 96-well plates and LDH activity was determined using a commercially available kit (LD-L50) from Sigma Diagnostics (St. Louis, MO, USA). The substrate/dye/enzyme (20 μl) mix was added to each well, the plates were covered with paper towels and shaken for 5 s. The plates were then stored in the dark for 20–30 min at room temperature before measuring the absorbance at 492 nm. The percent release of LDH was expressed as the units of LDH activity (U/L) in the medium of treated cells divided by the LDH activity units in the medium of untreated cells (× 100). LDH activity was calculated as

$$\text{LDH}(U/L) = ((\text{test OD–contrast OD})/(\text{standard OD–blank OD})) \times 0.2 \times 1000 \quad (3)$$

2.4.6. Annexin V-FITC/propidium iodide assay

Apoptosis-mediated cell death of tumor cells was examined using a FITC-labeled Annexin V/propidium iodide (PI) apoptosis detection kit (Molecular Probes, OR, USA) according to the manufacturer's instructions. After inducing apoptosis in the cells using PEP and controls, the cells were harvested by trypsinization, washed in PBS, centrifuged at 2000 rpm for 5 min and resuspended in 195 μl binding buffer (10 mM HEPES, 140 mM NaCl, 2.5 mM CaCl2, pH 7.4). On mixing the buffer with 5 μl Annexin V-FITC, the sample was incubated in the dark for 15 min at room temperature and thereafter centrifuged at 2000 rpm for 5 min. The supernatant was later removed, the cells were resuspended in 190 μl binding buffer and 5 μl of propidium iodide (PI) was added for detection. A minimum of 1×10^6 cells/ml were analyzed using a BD FACS Calibur flow cytometer (Becton Dickinson, CA, USA) within 30 min after supravital staining.

2.4.7. Cellular morphology analysis

Changes in cell morphology were determined as described by Hsu et al. (2011) with slight modifications. Cell suspension (100 μl in DMEM) was inoculated into each well of 96-well plates at 2×10^5 cells/well and incubated for 24 h. Next, the medium was removed and the cells were incubated with 100 μl of PEP or controls for 24 h. Morphological changes were observed and recorded using a microscope digital eyepiece camera (Ou Pulin OPLENIC, Hangzhou, P.R. China) mounted onto an inverted phase-contrast light microscope at 20 × magnification.

2.5. Immunostimulation

2.5.1. Proliferation of macrophages

Macrophage proliferation was determined using MTT, alamar blue, trypan blue, LDH, Annexin V-FITC/propidium iodide and morphological assays as described in Sections 2.4.1., 2.4.2., 2.45.3., 2.4.5., 2.4.6. and 2.4.7 respectively, using LPS (5 μg/ml) as the positive control.

2.5.2. Nitric oxide (NO) production

The NO released by macrophages was measured by determining the amount of accumulated nitrite (NO_2^-) in cell free supernatants via the Griess reaction (Jacobo-Salcedo et al., 2013; Krifa et al., 2013). Cells (2×10^5 cells/ml) were suspended in DMEM in 96-well culture plates and were incubated for 48 h at 37 °C and 5% CO_2. Thereafter, 100 μl of media from each well was aspirated, replaced with the same amount of fresh media, and further incubated for 48 h with different concentrations of PEP (0–160 μg/ml). LPS (5 μg/ml) was used as the positive control. Cell free supernatant (100 μl) was then mixed with an equal volume of the Griess reagent at room temperature for 10 min. Absorbance was determined at 540 nm in a microtiter plate reader and NO was estimated using a sodium nitrite standard curve. Results were presented as means obtained from mean OD of triplicate wells of each group and were expressed as μM.

2.5.3. Hydrogen (H_2O_2) peroxide release

Release of H_2O_2 by macrophages was determined according to Alonso-Castro et al. (2012). Cell culture supernatants (100 μl) of macrophages were mixed with equal volumes of fresh phenol red solution in 96-well plates and incubated for 3 h. Reaction was stopped by adding 10 μl 1N NaOH solution and the absorbance was spectrophotometrically read at 620 nm. Concentration of H_2O_2 was then determined by a standard curve of H_2O_2 (0–40 μM) and was expressed as μM.

2.5.4. Lysosomal enzyme activity

Cellular lysosomal enzyme activity was used to determine acid phosphatase (AcP) activity in macrophages as described by Jacobo-Salcedo et al. (2013) with modifications. Briefly, macrophage suspensions (100 μl aliquot of 6×10^6 cells/ml) were seeded into 96-well plates, treated with different concentrations of PEP (0–160 μg/ml) and incubated for 48 h. The medium was discarded and 20 ml of 0.1% Triton X100 (Sigma, St. Louis, MO), 100 ml of 100 mM *p*-nitrophenyl phosphate solution and 50 ml of citrate buffer (pH 5.0, 0.1 M) were added to each well. The plates were further incubated for 30 min before 150 ml of borate buffer (pH 9.8, 0.2 M) was added to each well. The absorbance was read at 405 nm and the percentage of lysosomal enzyme activity was calculated as

$$\text{Lysosomal enzyme activity}(\%) = 100 \times (\text{OD sample} - \text{OD negative control})/\text{OD negative control} \quad (4)$$

2.5.5. Pinocytosis

The pinocytic activity of PEP was evaluated using the neutral red assay as described by del Carmen Juárez-Vázquez et al. (2013) with slight modifications. Following the treatment of macrophages with PEP and control for 48 h, the culture medium was discarded, 200 μl of 0.7% neutral red was added into each well of a 96-well plate and cultured for another 1 h. The supernatant was then discarded and each well was washed with PBS. Lysing solution (200 μl, 0.1 M acetic acid: alcohol = 1:1) was lastly added to each well and the plates were kept overnight at 4 °C. The absorbance at 492 nm was read with PBS serving as a blank.

2.6. Statistics analysis

The results shown were from at least three independent experiments and were expressed as mean ± standard deviation (SD). They were subjected to a one-way analysis of variance (ANOVA) followed by a *t*-test for multiple comparisons. For a single comparison, the significance of differences between the means was determined by the Student's *t*-test. $P < 0.05$ was considered as statistically significant. All computations were done using statistical software (SAS, version 8.0).

3. Results

3.1. Extraction, purification and partial characterization

After extraction and purification through DEAE-52, CM-52 and Superdex 75 columns, a pure form of PEP was obtained (Fig. 1A–C). It was then applied to high-performance gel-permeation chromatography (HPGPC) for purity and molecular weight determination.

HPGPC has been shown to be an effective method for homogeneity and molecular weight determination. Therefore, it was utilized in our study to determine the purity and molecular weight of PEP, which yielded a single and symmetrically sharp peak (Fig. 2A). The developed calibration curve correlated the molecular weight with the HPGPC retention time of the standards, and was subsequently used for molecular weight evaluation. The molecular weight-retention time equation developed by the calibration curve was $\log Mw = 8.011 - 0.429t$ with $R^2 = 0.997$ (where *M*w was the average molecular weight of the sample and *t* was the sample's retention time). The HPGPC retention time for PEP was 7.49 min. Based on the molecular weight-retention time equation, PEP therefore had a molecular weight of about 63 kDa.

The infrared spectrum of PEP showed a broad peak in the range of 3600–3200 cm^{-1} and other obvious absorption peaks at 1654 and 1577 cm^{-1} (Fig. 2B). A significant resonance emerged at 3.9–4.5 ppm in the ^1H –NMR spectrum (Fig. 2C). Moreover, sharp intense peak at 4.7 ppm and multiple small peaks at 4.9 to 5.7 ppm were observed.

3.2. Cytotoxicity assays

3.2.1. MTT, AB, TB and NR assays

According to MTT assay results, the IC_{50} for A549, BGC-823 and HepG2 were 229.0 ± 1.24, 41.2 ± 1.1 and 36.5 ± 0.84 μg/ml respectively (Fig. 3A). PEP toxicity was least on HGC-27 and highest on HepG2 cells. Compared to PEP, the conventional cancer drugs demonstrated greater toxicity at even low concentrations (Fig. 3B–E).

Based on AB assay, inhibitory effects on cell viability were dependent on PEP concentrations (Fig. 4A). At IC_{50} PEP significantly inhibited 48.88 ± 1.22, 49.28 ± 0.74 and 49.05 ± 0.6% of A549, BGC-823 and HepG2 cells respectively. However, only at the highest concentration did PEP has a significant ($P < 0.05$) inhibition (21.93 ± 1.00) in HGC-27 cells (Fig. 4A). Additionally,

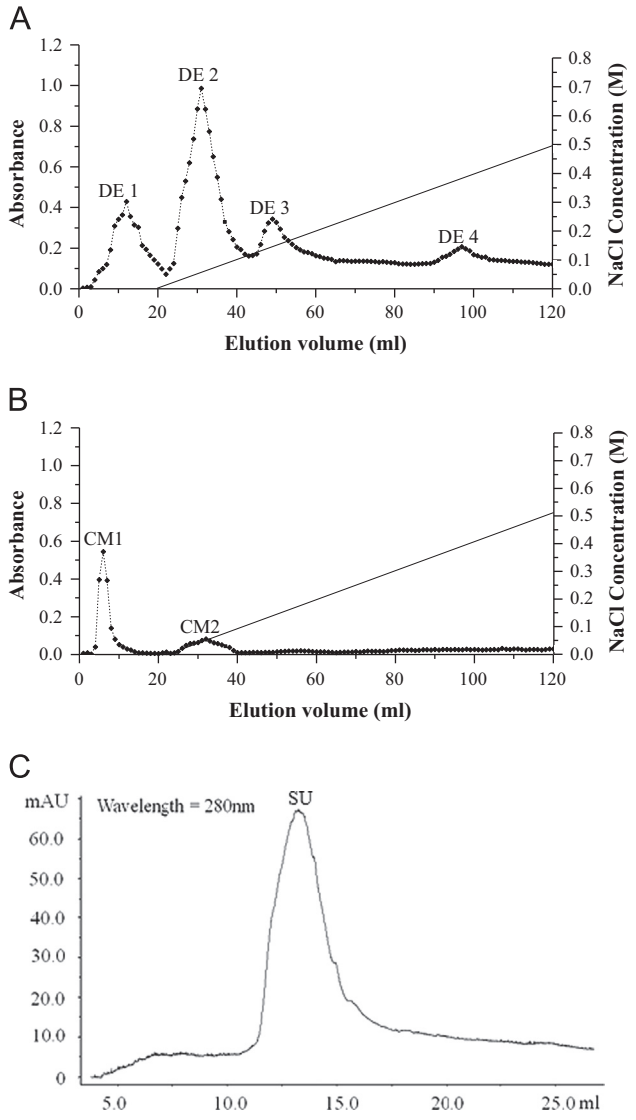

Fig. 1. Protein elution profile. (A) Anion-exchange chromatography of *Pleurotus eryngii* crude powder on a DEAE-52 column. (B) Cation-exchange chromatography of DE 2 on a CM-52 column (C) CM 1 gel filtration on a Superdex 75 column by FPLC on an ÄKTA Purifier System.

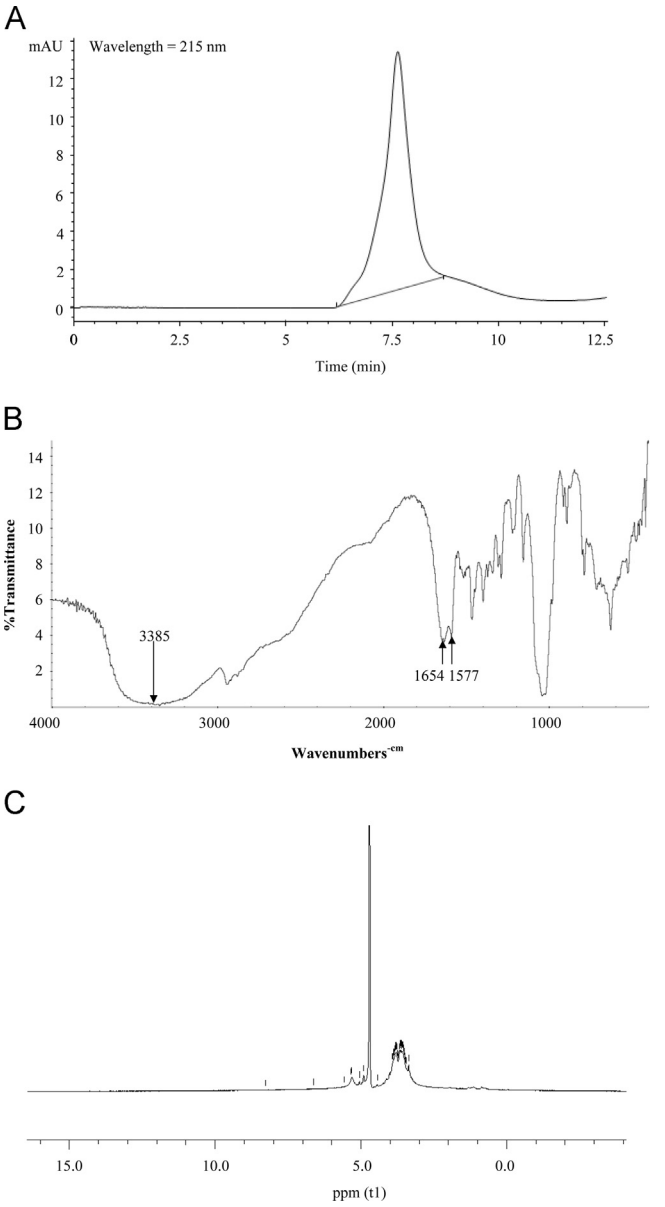

Fig. 2. (A) Purity and molecular weight determination of PEP on HPGPC. (B) FT-IR and (C) ^{1}H –NMR spectra of PEP.

remarkable cytotoxicity was observed in HepG2 cells with approximately 60% inhibition recorded at 320 μg/ml.

As indicated by TB assay results, plasma membrane damage was negligible at lower PEP concentrations but at higher concentrations (320 μg/ml), it increased to 29.64 ± 1.77, 31.49 ± 2.15, 24.77 ± 2.05 and 19.03.03 ± 0.75% for A549, BGC-823, HepG2 and HGC-27 cells respectively (Fig. 4B). The basic NR dye distributes to the acidic compartments in the cell and therefore acts as a marker for the integrity of lysosomes and possibly the Golgi apparatus (Varma et al., 2013). A sharp increase in percent toxicity occurred, with up to 23.12 ± 1.15% cell (HepG2) survival rate at the highest concentration (Fig. 4C). Remarkably, lowest concentration (40 μg/ml) also resulted in significantly ($P < 0.05$) higher inhibition values of 29.26 ± 1.54, 50.37 ± 2.18, 65.99 ± 1.21 and 23.83 ± 1.01% in A549, BGC-823, HepG2 and HGC-27 cells respectively.

3.2.2. Cell membrane integrity

Release of lactate dehydrogenase (LDH) in the media by apoptotic/necrotic cells was quantified and a concentration-dependent response was observed when the tumor cells were exposed to PEP (Fig. 4D). At the highest concentration, PEP resulted in a 13.36 ± 1.13, 24.51 ± 1.23, 30.23 ± 1.14 and 10.97 ± 1.00% increase of LDH leakage in A549, BGC-823, HepG2 and HGC-27 cells compared to the untreated cells, respectively (Fig. 4D).

3.2.3. Annexin V-FITC/PI staining

Annexin V/PI staining and flow cytometric analysis were used to determine PEP induced phosphatidylserine externalization, which is an early biomarker of apoptosis induction and increased membrane permeability, which indicate cell death. The percentage of early apoptotic cells (Annexin V^{+}/PI^{-}) ranged from 6.13% to 25.36% while late apoptotic cells (Annexin V^{+}/PI^{+}) ranged from 5.05% to 10.35% on treatment of tumor cells with PEP. However proliferation of RAW 264.7 cells did not change significantly (Fig. 5A).

3.2.4. Morphological characterization

On exposure to PEP, tumor cells shrunk, vacuolated, plasma membrane blebs and detachment occurred gradually as the

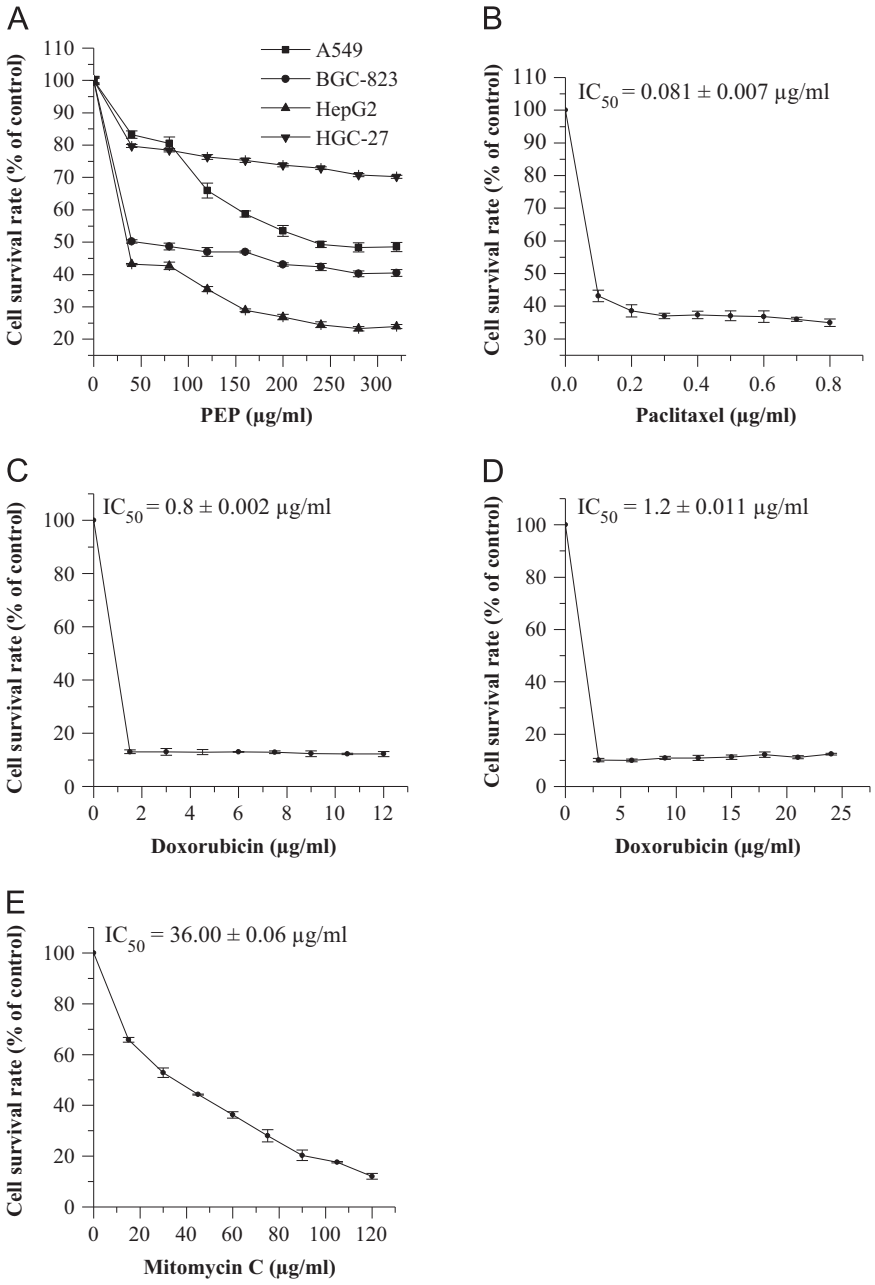

Fig. 3. (A) Determination of IC_{50} of PEP in A549, BGC-823, HepG2 and HGC-27 cells. (B) IC_{50}s of paclitaxel on A549, (C) doxorubicin on BGC-823, (D) doxorubicin on HepG2 and (E) mitomycin C on HGC-27 evaluated through mitochondrial activity using the MTT assay.

concentration increased (Fig. 5B). However, the hallmarks of apoptosis such as irregular cytoplasm membrane, cytoplasmic vacuolation and chromatin condensation did not develop after treatment of RAW 264.7 cells with PEP (Fig. 5B). These observations were in agreement with MTT, AB, NR, TB, LDH, Annexin V/PI assay results.

3.3. *in vitro* immunostimulation

3.3.1. Proliferation, LDH release, lysosomal and pinocytic activity of macrophages

Based on MTT, AB and TB assays, PEP significantly ($P < 0.05$) stimulated macrophage proliferation by 12.9 ± 1.50, 17.35 ± 2.76 and 20.83 ± 1.84% respectively at 160 μg/ml (Fig. 6A). Notwithstanding, less than 0.01% of RAW 264.7 cells had PEP-associated membrane rupture in LDH assay (Fig. 6B).

Lysosomal enzyme activity of macrophages was stimulated by PEP in a concentration-dependent manner, but with lower potency than LPS (Fig. 6C). At increasing PEP concentration, the lysosomal enzyme activity of RAW 264.7 cells increased by 21.89 ± 2.82% compared to the untreated cells (Fig. 6C). Pinocytic function of macrophages was measured by quantitative determination of neutral red dye in the cells. At 160 μg/ml pinocytosis of PEP-treated macrophages increased by 25.93 ± 1.1% compared to the untreated macrophages after 48 h of incubation (Fig. 6C).

3.3.2. Nitric oxide (NO) and hydrogen peroxide release

PEP-treated macrophages displayed a significant dose-dependent NO production increase (Fig. 6D). As PEP concentration increased

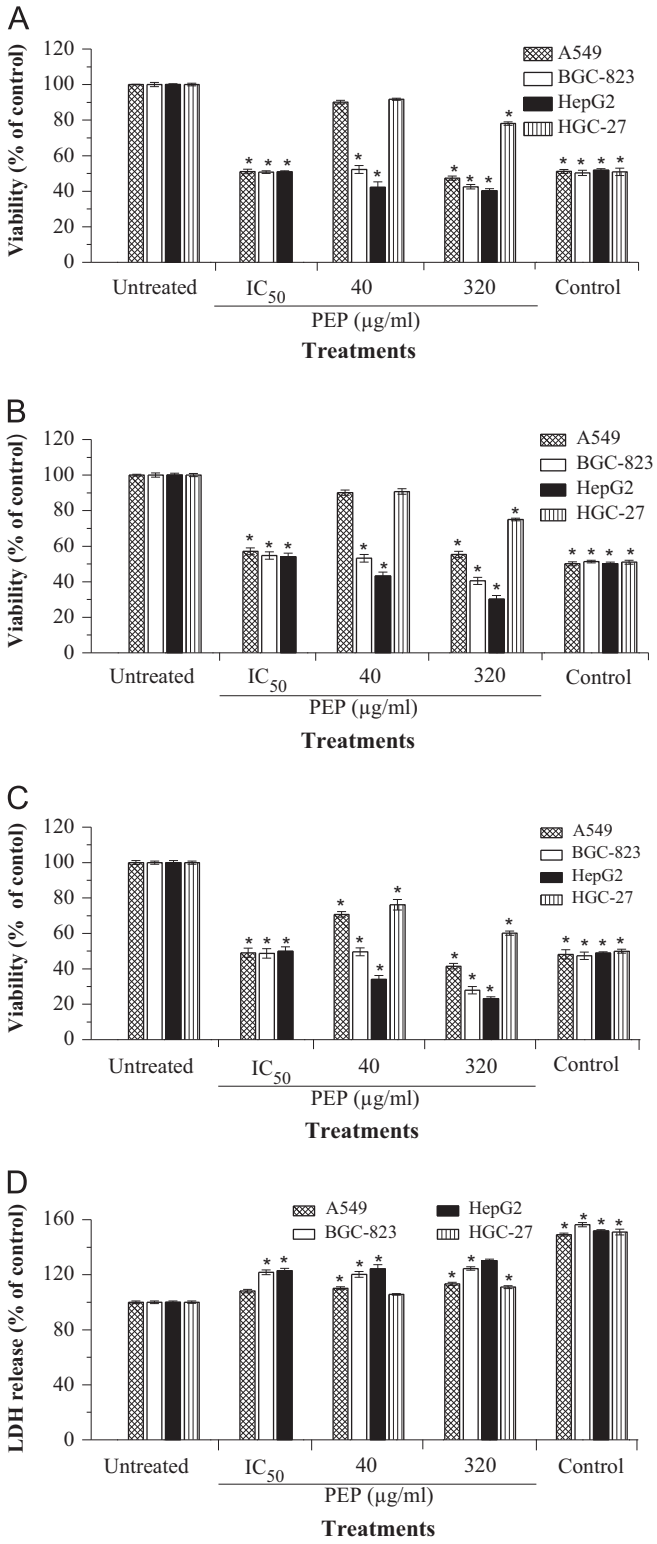

Fig. 4. PEP inhibits proliferation of A549, BGC-823, HepG2, HGC-27 cells dose-dependently. (A) Alamar blue assay. (B) Trypan blue assay. (C) Neutral red assay. (D) LDH assay. *$P < 0.05$ compared to untreated control group (100%).

from 0 to 160 μg/ml, NO release increased significantly ($P < 0.05$) from 5.6 ± 0.11 μM to 8.91 ± 0.67 μM respectively (Fig. 6D). Likewise, as concentration of PEP increased from 0 to 160 μg/ml, H_2O_2 release increased significantly ($P < 0.05$) from 3.5 ± 0.04 μM to 10.01 ± 0.52 μM respectively. When tested at 160 μg/ml, PEP showed a higher potency than LPS (Fig. 6D).

4. Discussion and conclusion

After the last purification step on Superdex 75 (Fig. 1C), the purity and molecular weight of PEP were confirmed using HPGLC which yielded a single symmetrical peak (2A), demonstrating homogeneity. From HPGLC results, PEP had a molecular weight of 63 KDa. PEP had a higher molecular mass than the previously reported proteins from *Pleurotus eryngii* and other oyster mushrooms. Antifungal peptides designated as eryngin and pleureryn with molecular masses of 10 kDa (Wang and Ng, 2004) and 11.5 kDa (Wang and Ng, 2001) have been isolated from the fruiting bodies of *Pleurotus eryngii*. A novel hemolysin has also been isolated from the edible mushroom *Pleurotus nebrodensis* (Lv et al., 2009). The hemolysin, nebrodeolysin, a monomeric protein with a molecular weight of approximately 27 kDa, exhibited hemolytic activity towards rabbit erythrocytes. It also showed cytotoxicity against HepG2 and HeLa cells. In general, high molecular weight biomolecules have been shown to exhibit higher bioactivity (Enshasy and Hatti-Kau, 2013). This therefore infers that PEP would possess greater biological activity than the reported molecules.

The intense band at 3385 cm^{-1} represented the stretching vibration of N–H (Fig. 2B). Peaks ranging from 3000 to 2800 cm^{-1} represent the vibrating absorption of the expanding and contracting N–H in the protein (Guo et al., 2013). Amide I and II are the two major bands of a protein infrared spectrum. Amide I band is in the region of 1600 and 1700 cm^{-1} and is mainly associated with the C═O (70–85%) and C–N (10–20%) groups stretching vibration (Guo et al., 2013). Amide II band is between 1510 and 1580 cm^{-1} wavenumbers and it corresponds to N–H bending at 40–60% (de Campos Vidal and Mello, 2011). In our IR spectrum results, peak 1577 cm^{-1} corresponded to this band (Fig. 2B). Besides, correspondence between the peak frequency of the amide I band and the secondary structure of protein has been well known where α-helices give rise to a main absorption band close to 1655 cm^{-1} (Barth, 2007). Thus, FT-IR spectral data suggested that the isolated protein connoted a secondary (α-helix) structure.

According to NMR spectrum (Fig. 2C), the broad multiply signal at 3.9–4.5 ppm in the aliphatic region corresponded to CH–O, which was mainly attributed to H_α of glycine (Zainuddin et al., 2008). Moreover, the intense and sharp peak at 4.7 ppm corresponded to N–H and was mainly attributed to arginine, while the smaller peaks appearing at 4.9–5.7 ppm corresponded to OH and were mainly attributed to serine (Zainuddin et al., 2008). The appearance of few very narrow peaks in the NMR spectra (3.4, 4.4, 4.9 and 5.1 ppm) suggested that PEP contained small portion of low molecular weight peptides which were free from hydrogen bonding. FT-IR and NMR analyses results therefore implied that PEP was a secondary α-helical protein, mainly composed of arginine, glycine and serine.

Naturally occurring compounds present in human diets have utmost significance in promoting and maintaining health, especially, those with low toxicity to normal cells. These compounds include phenols, resveratrol, curcumin and antioxidant peptides. Phenols have been shown to have antioxidant activity (Shahidi and Zhong, 2010) and antiproliferative activity against colorectal and lung cancer (Di Domenico et al., 2012). Equally, resveratrol has been found to be an active antioxidant and toxic to malignant gliomas and hepatocellular carcinoma cells (Colagiuri et al., 2013). Cytotoxicity of curcumin against cervical cancer cells has also been reported (Di Domenico et al., 2012) while antioxidant peptides have been shown to prevent and treat different disorders, such as arthrosclerosis, cancer, diabetes mellitus, and coronary heart (Shahidi and Zhong, 2010). Owing to their non-toxicity and potent biopharmacological activity, metabolites derived from mushrooms have received increasing attention in cancer therapy. More interestingly, antitumor activity of extracts from *Pleurotus eryngii* fruiting bodies on mice bearing renal cancer

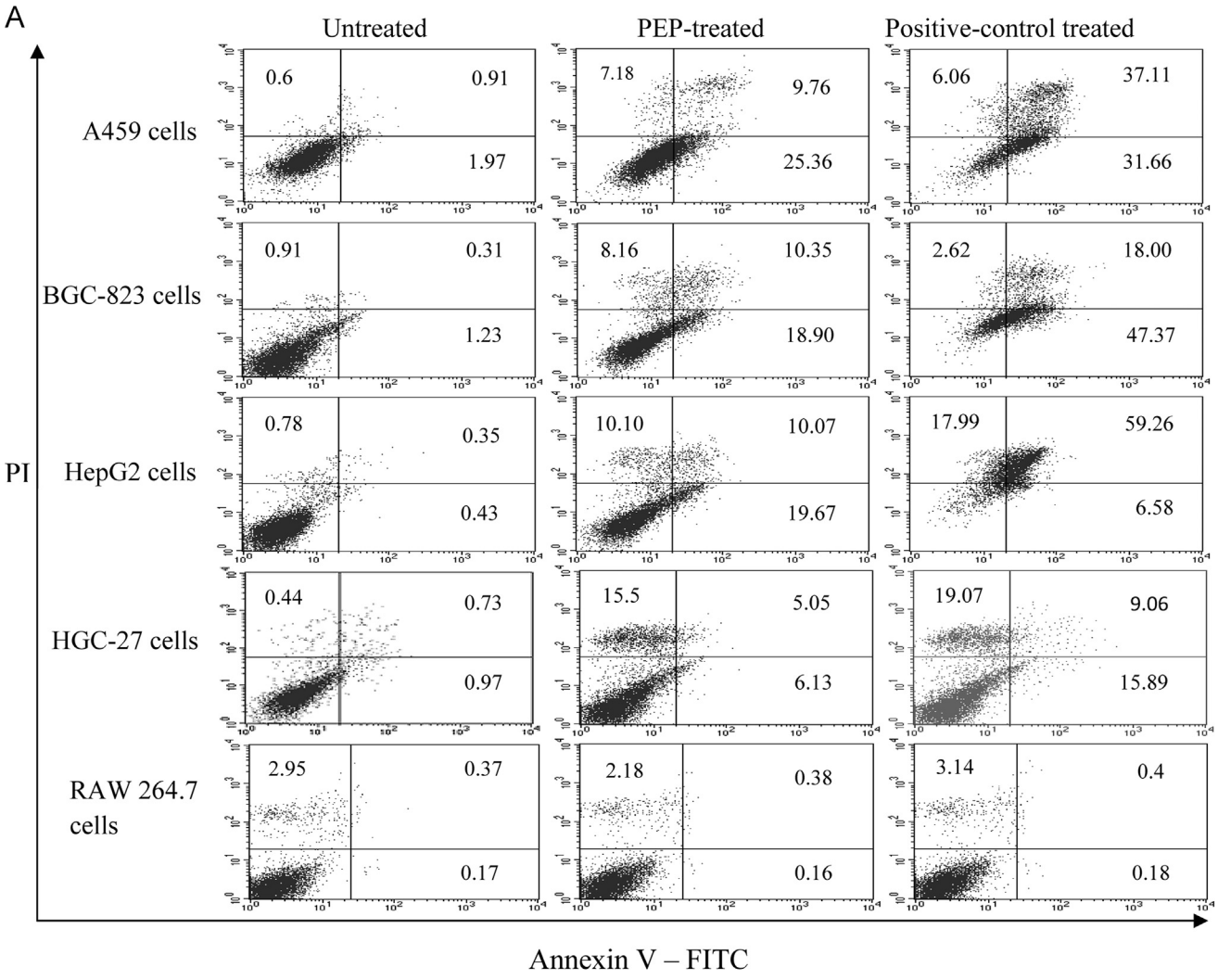

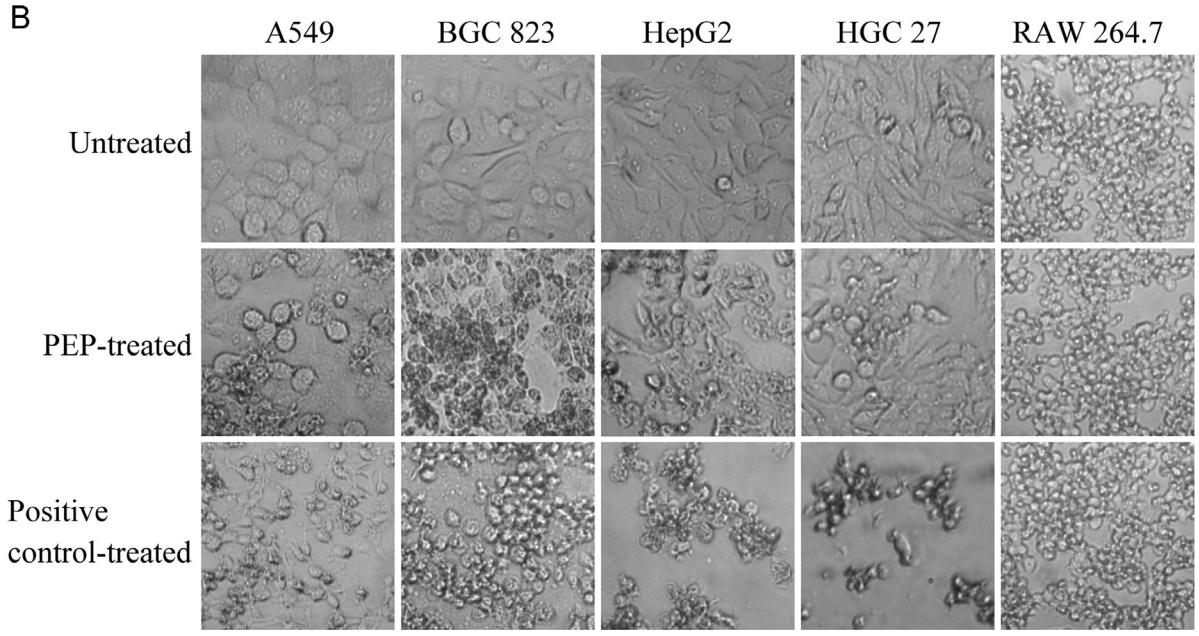

Fig. 5. (A) Contour diagram of FITC-Annexin V/PI flow cytometry of A549, BGC-823, HepG2 and HGC-27 after 24 h. The lower left quadrants of each panel show the viable cells, FITC-Annexin V^-/PI^-. The upper right quadrants contain the non-viable, necrotic cells, FITC-Annexin V^+/PI^+, uptake. The lower right quadrants represent the apoptotic cells, FITC-Annexin V^+/PI^-, demonstrating cytoplasmic membrane integrity. One representative experiment out of three is shown. (B) Morphological cellular examination of A549, BGC-823, HepG2, HGC-27 and RAW 264.7 cells.

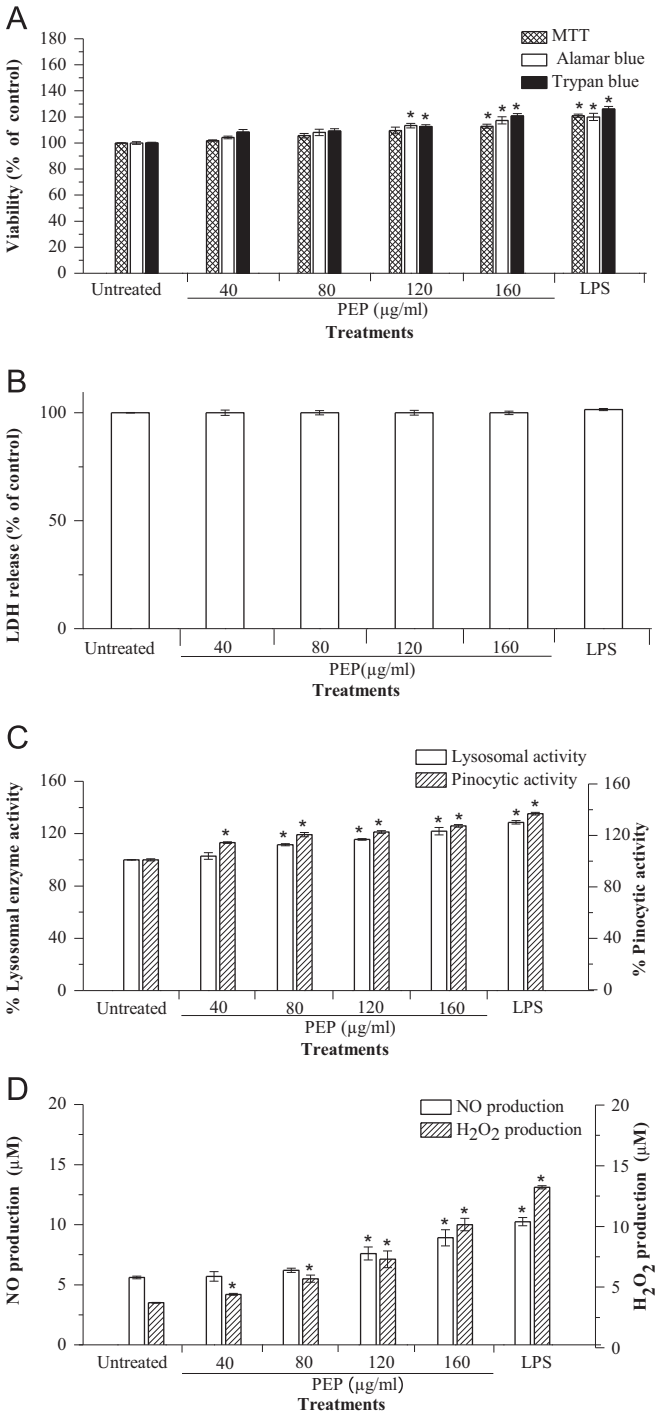

Fig. 6. PEP induces immunostimulatory effects in vitro. (A) MTT, Alamar blue and trypan blue assays. (B) LDH release. (C) Cellular lysosomal enzyme activity and pinocytic activity. (D) NO and H_2O_2 production. Data are representative of three independent experiments in hexaplicate. Results represent the mean ± standard deviation. *$P < 0.05$ compared to untreated control group.

has been reported (Yang et al., 2013). A hemolytic protein from *Pleurotus nebrodensis* mushroom with apoptosis-inducing and anti-HIV-1 effects has also been reported (Lv et al., 2009). Studies have also reported that an extract from *Pleurotus pulmonarius* can suppress liver cancer development and progression through inhibition of VEGF-induced PI3K/AKT signaling Pathway (Bauer et al., 2012).

Cell viability assays are vital steps in determining the cellular response to a toxicant, hence giving information on cell death, survival and metabolic activities (Deng et al., 2013). In this study, the assays were conducted using the PEP obtained from the fruiting bodies powder of *Pleurotus eryngii*. Based on the cytotoxicity assays results (Figs. 3–5), the possibility of the existence of more than one potential target of PEP toxicity in tumor cells, some more susceptible to PEP-associated damage than others was demonstrated. Data showed that NR assay was the most sensitive in revealing PEP-associated cytotoxicity in the tumor cells (Fig. 4C). Nonetheless, mitochondrial and cytosol damages seemed to be intermediate features whereas, plasma membrane damage was a late feature of PEP cytotoxicity. NR assay results suggested that in tumor cells, lysosomes readily interacted with the PEP (Fig. 4C). Based on NR results, we propose that intralysosomal localization of PEP may have led to damage of the lysosomal membranes, with ensuing leak to the cytosol of lytic enzymes, resulting in autolysis and apoptotic loss of viability. Lysosomes, also known as “suicidal bags” are highly vibrant membrane-bound organelles that act as the terminal degradative compartment of the endocytic, phagocytic and autophagic pathways (Repnik and Turk, 2010; Varma et al., 2013). Lysosomal cathepsins (cysteine cathepsins and the aspartic cathepsin D) are enzymes enclosed in the lysosomes. They help to maintain the homeostasis of the cell's metabolism by participating in the degradation of heterophagic and autophagic material and are most commonly associated with cell death (Repnik and Turk, 2010). Thus, following PEP treatment, the lysosomal membranes were destabilized, the cathepsins were released into the cytosol and the lysosomal pathway of apoptosis was initiated (Repnik and Turk, 2010; Varma et al., 2013). Damage to the plasma membrane required high PEP concentrations, as shown by the TB exclusion assay (Fig. 4B). The results showed that plasma membrane was resistant to PEP damage in all cancer cells thus, high concentrations of PEP were required before any significant damage to the plasma membrane occurred. In conclusion, we showed that in tumor cells the lysosomes/Golgi apparatus were most sensitive to PEP-mediated toxicity as reflected by the significantly higher percent toxicity values in the NR assay (Fig. 4C).

Determination of LDH leakage gives an idea on the viability of cells. This assay is based on the measurement of LDH activity in the extracellular medium. The loss of intracellular LDH and its release into the culture medium is an indicator of irreversible cell death due to cell membrane damage (Biswas et al., 2013). Our results showed that exposure to PEP induced significant membrane damage in tumor cell with HepG2 cells being the most sensitive, having up to 30% LDH increase at 320 μg/ml (Fig. 4D). The LDH leakage assay results were in good agreement with TB assay results (Fig. 4B). Nevertheless, LDH release assay is not only used to indicate cytotoxicity, but also to measure cell necrosis and apoptosis (Zhang et al., 2008). Hence, the increase in LDH released from the cells with increasing PEP concentrations suggested that the exposure of cells to PEP may have induced necrosis or apoptosis, consequently decreasing their viability (Fig. 4D).

Apoptosis has been recognized as the principal mechanism by which chemotherapeutic agents and radiotherapy kill cancer cells. Apoptosis can be triggered by various forms of physiologic stimuli or stresses, such as cytokines, free radicals and DNA damage (Zhou et al., 2012; Chen et al., 2013). Apoptotic cells represent membrane alterations, like transfer of phosphatidylserine from the inner side of the plasma membrane to the outer layers (Zhou et al., 2012). Annexin V is a recombination protein that specifically binds to phosphatidylserine residues with high affinity. It can be combined with specific membrane-impermeant nucleic acid dyes to discriminate apoptosis from necrosis (Zhou et al., 2012). To validate the cytotoxicity results, flow cytometry analysis based on Annexin V-FITC/PI staining was conducted and apoptosis was effectively induced within 24 h of PEP treatment (Fig. 5A). Although positive controls-induced cytotoxicity was higher in cancer cells than PEP

cytotoxicity, early apoptotic cells (Annexin V^+/PI^-) increased significantly ($P < 0.05$) from 0.43% in untreated tumor cells group to 25.36% in PEP-treated group (Fig. 5A). This indicated that induction of apoptosis accounted for the growth retardation of the tumor cells after the treatment with PEP as confirmed by MTT, AB, TB and NR results. Furthermore, PEP might have affected the expression of proteins involved in the apoptotic process of the tumor cells. Treatment of A549, BGC-823, HepG2 and HGC-27 cells with PEP may have caused an increase in the levels of p53, a protein involved in apoptosis (Vaz et al., 2012). Based on the results, this effect was cell- and concentration-dependent. The levels of p21, whose expression is regulated by p53 and is related to cell cycle arrest (Ding et al., 2012), might have been also elevated. Anticancer agents may alter regulation of the cell cycle machinery, resulting in cellular arrest at different phases of the cell cycle and, thereby, reducing the growth and proliferation of, and even inducing apoptosis in cancerous cells (Hseu et al., 2008). Apoptosis is detected as a sub-G_0/G_1 peak in the cell cycle analyses (Ding et al., 2012). Thus, given the apoptotic results, PEP might have induced expression of p53 and sub-G_0/G_1 cell cycle arrest hence inhibiting cell proliferation.

Morphological examination results (Fig. 5B) demonstrated transformation of tumor cells that had interacted with PEP into floating (detached), shrunken cells with long and slender processes, blebbed cytoplasm and condensed nuclei deducing apoptosis (Chen et al., 2013). This corroborated the MTT, AB, TB, NR, LDH and Annexin V-FITC/PI results. However, there were no notable morphological changes in RAW 264.7 cells indicative of apoptosis.

The immune system is the human's ultimate defense against infectious diseases, tumor and cancer growth (Krifa et al., 2013). The fight against cancer cells in the human body involves a defense system that is comprised of the innate and adaptive immunities. This system is controlled by a series of immune responses mediated by different immune cells and their secretory substances including cytokines, chemokines, NO and H_2O_2 (Wong et al., 2011). In cancer treatment, chemo- and radiotherapy are always accompanied by immunosuppression (Alonso-Castro et al., 2012; Yang et al., 2013). Therefore, it is inevitable to find new antitumor regimens with potential to stimulate the immune system. It is well known that macrophages play a crucial role in cellular defense mechanisms against pathogens, tumor and cancer growth through phagocytosis, synthesis and release of NO and H_2O_2 (Pinheiro et al., 2013). Activated macrophages characteristically demonstrate increased membrane ruffling, increased adhesion and spreading. There is also stimulation of DNA synthesis, modified monokine secretion, increased NO and H_2O_2 release, elevated lysosomal enzyme levels, altered phagocytic activity and increased bactericidal/tumoricidal activity (Alonso-Castro et al., 2012). Phagocytosis, a mechanism by which cells internalize, degrade and eventually present peptides derived from particulate antigens in order to defend the body, is very prominent in macrophages and is critical for their functions (Lopes et al., 2006). In this study, we showed that PEP enhanced macrophage spreading and proliferation (Fig. 5B and Fig. 6A respectively). It was also less toxic to the cell membranes of macrophages (Fig. 6B). Additionally, PEP stimulated lysosomal enzyme and pinocytic activities (Fig. 6C), and NO and H_2O_2 release (Fig. 6D) comparably with LPS. Lysosomes and endosomes are both implicated in macrophage killing ability (Repnik and Turk, 2010). Increase in lysosomal enzyme activity is accompanied by the release of lysosomal enzymes like acid phosphatase (AcP) that are used for the killing and digesting of microbial pathogens through phagocytosis (Nandakumar et al., 2011). The higher the AcP activity, the greater the phagocytic stimulation and intracellular killing capacity (Repnik and Turk, 2010). Besides, the NR dye uptake assay is based on the ability of viable cells to incorporate and bind this dye in their lysosomes via active transport hence quantifying the pinocytic ability of macrophages (del Carmen Juárez-Vázquez et al., 2013). Based on lysosomal enzyme activity and NR uptake assay results, we can infer that PEP also targeted lysosomes in the macrophages where it induced phagocytic and pinocytic activities of the cells. Moreover, NO is an important signaling molecule synthesized from L-arginine by NO synthase in immunoreactive cells and is known to play key roles including bactericidal and tumoricidal functions (Krifa et al., 2013). Indeed, a major role of NO is to mediate bactericidal and tumoricidal actions of activated macrophages (Son et al., 2006). The current study demonstrated that PEP has an inductive effect on the macrophage activation leading to NO production. Therefore, the PEP-stimulated macrophages would have the potential to eliminate transformed cells and infectious pathogenic microorganisms. Additionally, PEP-mediated NO production would have signaled movement, proliferation (Fig. 6A), pinocytosis (Fig. 6C) and phagocytosis in macrophages thus enhancing their immune function. On treating macrophages with PEP, H_2O_2 production was significantly increased. After interaction with particles or certain soluble stimuli, phagocytic cells strongly enhance their consumption of oxygen and release superoxide anion, which rapidly undergoes dismutation into H_2O_2. H_2O_2 is considered a major factor in macrophage-mediated cytotoxicity and parasite killing (Arany et al., 2004). Therefore, it is probable that PEP would affect the expression of a number of various biological factors including H_2O_2 playing a key role in host defense, such as immunity to infections and anti-cancer activity.

In conclusion the present study showed that PEP was not only cytotoxic to tumor cells, but also had different organelle targets in the cells. However, the isolated *Pleurotus eryngii* protein was less toxic, it stimulated the proliferation, lysosomal enzyme and pinocytosis activities, nitric oxide and hydrogen peroxide release in macrophage, RAW 264.7 cells. This confirmed that PEP was not only toxic to tumor cells but also activated the macrophage-mediated immune responses. Hence, *Pleurotus eryngii* fruiting bodies powder is an active antitumor agent with immunomodulatory activity, where, it targets the lysosomes of cancerous cells concomitantly stimulating macrophage-mediated immune response.

Acknowledgment

The authors acknowledge financial support from China Agriculture Research System (CARS-24).

References

Alonso-Castro, A.J., Ortiz-Sánchez, E., Domínguez, F., Arana-Argáez, V., Juárez-Vázquez, M.d.C., Chávez, M., García-Carrancá, A., 2012. Antitumor and immunomodulatory effects of *Justicia spicigera* Schltdl (Acanthaceae. Journal of Ethnopharmacology 141 (3), 888–894, http://dx.doi.org/10.1016/j.jep.2012.03.036.

Arany, I., Megyesi, K., Kaneto, H., Tanaka, S., Safristein, R., 2004. Activation of ERK or inhibition of JNK ameliorates H2O2 cytotoxicity in mouse renal proximal tubule cells. Kidney International 65, 1231–1239.

Barth, A., 2007. Infrared spectroscopy of proteins. Biochimica et Biophysica Acta (BBA) – Bioenergetics *1767* (9), 1073–1101, http://dx.doi.org/10.1016/j.bbabio.2007.06.004.

Bauer, J.A., Xu, W., Huang, J.J.-h., Cheung, P.C.K., 2012. Extract of *Pleurotus pulmonarius* suppresses liver cancer development and progression through inhibition of VEGF-Induced PI3K/AKT signaling pathway. PLoS ONE *7* (3), e34406, http://dx.doi.org/10.1371/journal.pone.0034406.

Biswas, S., Deshpande, P.P., Perche, F., Dodwadkar, N.S., Sane, S.D., Torchilin, V.P., 2013. Octa-arginine-modified pegylated liposomal doxorubicin: an effective treatment strategy for non-small cell lung cancer. Cancer Letters *335* (1), 191–200, http://dx.doi.org/10.1016/j.canlet.2013.02.020.

Bradford, M.M., 1976. A rapid and sensitive method for quantitation of microgram quantities of protein utilizing the principle of protein-dye binding. Analytical Biochemistry *72*, 248–254.

Chang, H., Chien, P., Tong, M., Sheu, F., 2007. Mushroom immunomodulatory proteins possess potential thermal/freezing resistance, acid/alkali tolerance and dehydration stability. Food Chemistry *105* (2), 597–605, http://dx.doi.org/10.1016/j.foodchem.2007.04.048.

Chang, S.T., 1999. World production of cultivated edible and medicinal mushrooms in 1997 with empasis on *Lentinus edodes* (Berk) Sing. In china. International Journal of Medicinal Mushrooms *1*, 310–318.
Chen, G., Zhang, P., Huang, T., Yu, W., Lin, J., Li, P., Chen, K., 2013. Polysaccharides from *Rhizopus nigricans* mycelia induced apoptosis and G2/M arrest in BGC-823 cells. Carbohydrate Polymers *97* (2), 800–808, http://dx.doi.org/10.1016/j.carbpol.2013.05.068.
Chen, J., Mao, D., Yong, Y., Li, J., Wei, H., Lu, L., 2012. Hepatoprotective and hypolipidemic effects of water-soluble polysaccharidic extract of *Pleurotus eryngii*. Food Chemistry *130* (3), 687–694, http://dx.doi.org/10.1016/j.foodchem.2011.07.110.
Colagiuri, B., Dhillon, H., Butow, P.N., Jansen, J., Cox, K., Jacquet, J., 2013. Does assessing patients' expectancies about chemotherapy side effects influence their occurrence? Journal of Pain and Symptom Management *46* (2), 275–281, http://dx.doi.org/10.1016/j.jpainsymman.2012.07.013.
de Campos Vidal, B., Mello, M.L.S., 2011. Collagen type I amide I band infrared spectroscopy. Micron *42* (3), 283–289, http://dx.doi.org/10.1016/j.micron.2010.09.010.
del Carmen Juárez-Vázquez, M., Josabad Alonso-Castro, A., García-Carrancá, A., 2013. Kaempferitrin induces immunostimulatory effects in vitro. Journal of Ethnopharmacology *148* (1), 337–340, http://dx.doi.org/10.1016/j.jep.2013.03.072.
Deng, X., Zhang, F., Rui, W., Long, F., Wang, L., Feng, Z., Ding, W., 2013. PM2.5-induced oxidative stress triggers autophagy in human lung epithelial A549 cells. Toxicology in vitro *27* (6), 1762–1770, http://dx.doi.org/10.1016/j.tiv.2013.05.004.
Di Domenico, F., Foppoli, C., Coccia, R., Perluigi, M., 2012. Antioxidants in cervical cancer: chemopreventive and chemotherapeutic effects of polyphenols. Biochimica et Biophysica Acta (BBA) – Molecular Basis of Disease *1822* (5), 737–747, http://dx.doi.org/10.1016/j.bbadis.2011.10.005.
Ding, X., Zhu, F.-S., Li, M., Gao, S.-G., 2012. Induction of apoptosis in human hepatoma SMMC-7721 cells by solamargine from *Solanum nigrum* L. Journal of Ethnopharmacology *139* (2), 599–604, http://dx.doi.org/10.1016/j.jep.2011.11.058.
Enshasy, H.A.E., Hatti-Kau, R., 2013. Mushroom immunomodulators: unique molecules with unlimited applications. Trends in Biotechnology *31* (12), 668–677, http://dx.doi.org/10.1016/j.tibtech.2013.09.003.
Fujita, R., Liu, J., Shimizu, K., Konishi, F., Noda, K., Kumamoto, S., Kondo, R., 2005. Anti-androgenic activities of *Ganoderma lucidum*. Journal of Ethnopharmacology *102* (1), 107–112, http://dx.doi.org/10.1016/j.jep.2005.05.041.
Gunde-Cimerman, N., 1999. Medicinal value of the genus *Pleurotus* (Fr.) P. Karst. (Agaricales S.I., Basidiomycetes). International Journal of Medicinal Mushrooms *1*, 69–80.
Guo, H., Kimura, T., Furutani, Y., 2013. Distortion of the amide-I and -II bands of an α-helical membrane protein, pharaonis halorhodopsin, depends on thickness of gold films utilized for surface-enhanced infrared absorption spectroscopy. Chemical Physics *419*, 8–16, http://dx.doi.org/10.1016/j.chemphys.2012.11.011.
Hobbs, C., 1995. Medicinal Mushrooms: An Exploration of Tradition. Healing and Culture. Botanica Press, Santa Cruz, CA.
Hseu, Y.-C., Chen, S.-C., Chen, H.-C., Liao, J.-W., Yang, H.-L., 2008. *Antrodia camphorata* inhibits proliferation of human breast cancer cells in vitro and in vivo. Food and Chemical Toxicology *46* (8), 2680–2688, http://dx.doi.org/10.1016/j.fct.2008.04.036.
Hsu, H.-F., Huang, K.-H., Lu, K.-J., Chiou, S.-J., Yen, J.-H., Chang, C.-C., Houng, J.-Y., 2011. *Typhonium blumei* extract inhibits proliferation of human lung adenocarcinoma A549 cells via induction of cell cycle arrest and apoptosis. Journal of Ethnopharmacology *135* (2), 492–500, http://dx.doi.org/10.1016/j.jep.2011.03.048.
Jacobo-Salcedo, M.d.R., Juárez-Vázquez, M.d.C., González-Espíndola, L.Á., Maciel-Torres, S.P., García-Carrancá, A., Alonso-Castro, A.J., 2013. Biological effects of aqueous extract from Turkey vulture *Cathartes aura* (Cathartidae) meat. Journal of Ethnopharmacology *145* (2), 663–666, http://dx.doi.org/10.1016/j.jep.2012.11.014.
Jeong, Y.-T., Jeong, S.-C., Gu, Y.-A., Islam, R., Song, C.-H., 2010. Antitumor and immunomodulating activities of endo-biopolymers obtained from a submerged culture of *Pleurotus eryngii*. Food Science and Biotechnology *19* (2), 399–404, http://dx.doi.org/10.1007/s10068-010-0056-4.
Krifa, M., Bouhlel, I., Ghedira-Chekir, L., Ghedira, K., 2013. Immunomodulatory and cellular anti-oxidant activities of an aqueous extract of *Limoniastrum guyonianum* gall. Journal of Ethnopharmacology *146* (1), 243–249, http://dx.doi.org/10.1016/j.jep.2012.12.038.
Liang, Z-c, Wu, K-j., Wang, J-c, Lin, C-h, Wu, C-y., 2011. Cultivation of the Culinary-Medicinal Lung Oyster Mushroom, *Pleurotus pulmonarius* (Fr.) Quél. (Agaricomycetideae) on Grass Plants in Taiwan. International Journal of Medicinal Mushrooms *13* (2), 193–199.
Lopes, L., Godoy, L.M.F., de Oliveira, C.C., Gabardo, J., Schadeck, R.J.G., Buchi, D.d.F., 2006. Phagocytosis, endosomal/lysosomal system and other cellularaspects of macrophage activation by Canova medication. Micron *37* (3), 277–287, http://dx.doi.org/10.1016/j.micron.2005.08.005.
Lv, H., Kong, Y., Yao, Q., Zhang, B., Leng, F.-w., Bian, H.-j., Bao, J.-k., 2009. Nebrodeolysin, a novel hemolytic protein from mushroom *Pleurotus nebrodensis* with apoptosis-inducing and anti-HIV-1 effects. Phytomedicine *16* (2-3), 198–205, http://dx.doi.org/10.1016/j.phymed.2008.07.004.
Mizuno, T., 1995. Mushrooms: the versatile fungus – food and medicinal properties. Food Reviews International (Special issue) *2*, 1–235.
Mosmann, T., 1983. Rapid colorimetric assay for cellular growth and survival: application to proliferation and cytotoxicity assays. Journal of Immunological Methods *65*, 55–63.
Mukherjee, S.G., O'Claonadh, N., Casey, A., Chambers, G., 2012. Comparative in vitro cytotoxicity study of silver nanoparticle on two mammalian cell lines. Toxicology in vitro *26* (2), 238–251, http://dx.doi.org/10.1016/j.tiv.2011.12.004.
Nandakumar, N., Haribabu, L., Perumal, S., Balasubramanian, M.P., 2011. Therapeutic effect of hesperidin with reference to biotransformation, lysosomal and mitochondrial TCA cycle enzymes against 7,12-dimethylbenz(a)anthracene-induced experimental mammary cellular carcinoma. Biomedicine Aging Pathology *1* (3), 158–168, http://dx.doi.org/10.1016/j.biomag.2011.09.001.
Pareek, A., Godavarthi, A., Issarani, R., Nagori, B.P., 2013. Antioxidant and hepatoprotective activity of *Fagonia schweinfurthii* (Hadidi) Hadidi extract in carbon tetrachloride induced hepatotoxicity in HepG2 cell line and rats. Journal of Ethnopharmacology *150* (3), 973–981, http://dx.doi.org/10.1016/j.jep.2013.09.048.
Pinheiro, A.M., Santos, C.V.C.D., Rodrigues, L.E.A., 2013. *Neospora caninum*: infection induces high lysosomal activity. Experimental Parasitology *134* (4), 409–412, http://dx.doi.org/10.1016/j.exppara.2013.04.008.
Repnik, U., Turk, B., 2010. Lysosomal–mitochondrial cross-talk during cell death. Mitochondrion *10* (6), 662–669, http://dx.doi.org/10.1016/j.mito.2010.07.008.
Shahidi, F., Zhong, Y., 2010. Novel antioxidants in food quality preservation and health promotion. European Journal of Lipid Science and Technology *112* (9), 930–940, http://dx.doi.org/10.1002/ejlt.201000044.
Son, C.G., Shin, J.W., Cho, J.H., Cho, C.K., Yun, C.-H., Chung, W., Han, S.H., 2006. Macrophage activation and nitric oxide production by water soluble components of *Hericium erinaceum*. International Immunopharmacology *6* (8), 1363-–1369, http://dx.doi.org/10.1016/j.intimp.2006.03.005.
Synytsya, A., Míčková, K., Synytsya, A., Jablonský, I., Spěváček, J., Erban, V., Čopíková, J., 2009. Glucans from fruit bodies of cultivated mushrooms *Pleurotus ostreatus* and *Pleurotus eryngii*: structure and potential prebiotic activity. Carbohydrate Polymers *76* (4), 548–556, http://dx.doi.org/10.1016/j.carbpol.2008.11.021.
Taner, G., Aydın, S., Aytaç, Z., Başaran, A.A., Başaran, N., 2013. Assessment of the cytotoxic, genotoxic, and antigenotoxic potential of Pycnogenol® in in vitro mammalian cells. Food and Chemical Toxicology *61*, 203–208, http://dx.doi.org/10.1016/j.fct.2013.06.053.
Varma, H., Gangadhar, N.M., Letso, R.R., Wolpaw, A.J., Sriramaratnam, R., Stockwell, B.R., 2013. Identification of a small molecule that induces ATG5-and-cathepsin-l-dependent cell death and modulates polyglutamine toxicity. Experimental Cell Research *319* (12), 1759–1773, http://dx.doi.org/10.1016/j.yexcr.2013.03.019.
Vaz, J.A., Ferreira, I.C.F.R., Tavares, C., Almeida, G.M., Martins, A., Helena Vasconcelos, M., 2012. *Suillus collinitus* methanolic extract increases p53 expression and causes cell cycle arrest and apoptosis in a breast cancer cell line. Food Chemistry *135* (2), 596–602, http://dx.doi.org/10.1016/j.foodchem.2012.04.127.
Wang, H., Ng, T.B., 2001. Pleureryn, a Novel Protease from Fresh Fruiting Bodies of the Edible Mushroom *Pleurotus eryngii*. Biochemical and Biophysical Research Communications *289* (3), 750–755, http://dx.doi.org/10.1006/bbrc.2001.6037.
Wang, H., Ng, T.B., 2004. Eryngin, a novel antifungal peptide from fruiting bodies of the edible mushroom *Pleurotus eryngii*. Peptides *25* (1), 1–5, http://dx.doi.org/10.1016/j.peptides.2003.11.014.
Wasser, S.P., Weis, A.L., 1999. Medicinal properties of substances occurring in higher basidiomycetes mushrooms. Journal of Medicinal mushrooms *3*, 87–91.
Wasser, S.P., 2002. Medicinal mushrooms as a source of antitumor and immunomodulating polysaccharides. Applied Microbiology and Biotechnology *60* (3), 258–274, http://dx.doi.org/10.1007/s00253-002-1076-7.
Wiel, A., 1987. Mushroom a day. American Health *2*, 129–134.
Wong, K.-H., Lai, C.K. M., Cheung, P.C. K., 2011. Immunomodulatory activities of mushroom sclerotial polysaccharides. Food Hydrocolloids *25* (2), 150–158, http://dx.doi.org/10.1016/j.foodhyd.2010.04.008.
Yang, Z., Xu, J., Fu, Q., Fu, X., Shu, T., Bi, Y., Song, B., 2013. Antitumor activity of a polysaccharide from *Pleurotus eryngii* on mice bearing renal cancer. Carbohydrate Polymers *95* (2), 615–620, http://dx.doi.org/10.1016/j.carbpol.2013.03.024.
Zainuddin, Le, T.T., Park, Y., Chirila, T.V., Halley, P.J., Whittaker, A.K., 2008. The behavior of aged regenerated *Bombyx mori* silk fibroin solutions studied by 1H NMR and rheology. Biomaterials *29* (32), 4268–4274, http://dx.doi.org/10.1016/j.biomaterials.2008.07.041.
Zhang, X., Yang, F., Xu, C., Liu, W., Wen, S., Xu, Y., 2008. Cytotoxicity evaluation of three pairs of hexabromocyclododecane (HBCD) enantiomers on Hep G2 cell. Toxicology in vitro *22* (6), 1520–1527, http://dx.doi.org/10.1016/j.tiv.2008.05.006.
Zhou, C., Qian, L., Ma, H., Yu, X., Zhang, Y., Qu, W., Xia, W., 2012. Enhancement of amygdalin activated with β-d-glucosidase on HepG2 cells proliferation and apoptosis. Carbohydrate Polymers *90* (1), 516–523, http://dx.doi.org/10.1016/j.carbpol.2012.05.073.
Zhou, J., Chen, Y., Xin, M., Luo, Q., Gu, J., Zhao, M., Song, G., 2013. Structure analysis and antimutagenic activity of a novel salt-soluble polysaccharide from *Auricularia polytricha*. Journal of the Science of Food and Agriculture *93* (13), 3225–3230, http://dx.doi.org/10.1002/jsfa.6161.